DESIGN AND IMPLEMENTATION OF DUAL OUTPUT FORWARD CONVERTER TO POWER-UP DIGITAL UNIT FOR SPACE APPLICATION

Nikhil Kumar[1], A.N. Nagashree[2], Santosh B L[3], Prakash G[4], B K Singh[5]

[1]*M.Tech PE, Dept of EEE, BMSCE Bengaluru. nikhil.epe20@bmsce.ac.in*
[2]*Associate Professor and Head, Dept of EE,BMSCE. annagashree.eee@bmsce.ac.in*
[3]*Assistant Manager ,Centum Electronics Ltd, santoshbl@centumelctronics.com*
[4] *Engineer, Centum Electronics Ltd, prakashg@ centumelctronics.com*
[5]*Director, Centum Electronics Ltd.*

Abstract.

In recent years, DC-DC converters find many applications in low to medium power range. The isolated converters are used in medium power application since they provide isolation between input and output and protection from input side faults.This paper presents application of isolated DC-DC converter to power-up digital unit subsystem for space mission. The proposed converter is designed to operate at switching frequency of 140 kHz which reduces the size of magnetic components. The proposed topology uses a voltage feed forward control technique to adjust duty cycle for an input variation. It has a built in EMI filters to mitigate noise that emerge from surrounding components and vice versa. Meeting cross regulation is a challenging task and this is achieved by maintaining secondary feedback circuit in stable region. A prototype model is developed having Hybrid Micro Circuits (HMC) which reduces the size of the converter. It is aimed to achieve converter efficiency greater than 65%.

Keywords: DC-DC Converter, Forward Converter, Feed Forward, Mag-amp, LCD(Lossless) Snubber, UC2525 PWM controller.

1. INTRODUCTION

Nowadays, DC- DC converters are used in a range of applications from consumer electronics and telecommunications to industrial, medical and space. For space mission application, the most important requirements are high reliability and light weight design rather than conversion efficiency[1]. Though other topologies like full bridge, half Bridge and push pull DC-DC converters are capable of high efficiency but their reliability is low due to high side switch structure. Hence single switch forward converter with tertiary winding as demagnetizing or reset winding is used, as the converter is best suitable for low to medium power applications with high output currents. However, in single switch forward converter, reset winding is unable to put off leakage inductance spike, which may cause stress on the MOSFET switch. Therefore, this core has to be reset completely using an RCD snubber circuit consisting of resistor, capacitor and a diode. When the switch turns on the capacitor charges through diode and when the switch turns off it discharges stored energy into resistor. But the drawback of this method is, it decreases the efficiency

due to losses in the resistor [2]. To overcome this, LCD or lossless snubber is used as an alternative to RCD snubber which is non-dissipative in nature. It gives protection against dv/dt as well as di/dt. It is a challenging task to achieve good load regulation while designing the converter. So magnetic-amplifiers (Mag-amp) are used as post regulators on secondary side to maintain load regulation within the specification. The feedback control circuits for each output are used to achieve precise regulation of output voltages.

2. SPECIFICATIONS AND BLOCK DIAGRAM

The Forward Converter specifications are shown in Table 1

Table I. Forward Converter Specification

Parameters	Specification
Input Voltage	24V(min),36V(nom),42.5V(max)
Output-1	5.5V/12A
Output-2	5V/2A
Switching Frequency	140±5kHz
Efficiency	>65%
Output Power	76W
Ripple	<30mVp-p
Line Regulations	<±1%
Load Regulations	<±2%

The detailed block diagram of the proposed converter is shown in Fig 1. On the input side it has an EMI filter to reduce noise. Inrush current limiter circuit, limits the input current on application of ON command with 100% load to less than the twice of input current. Current sense circuit protects the converter from over current or short circuit current. It uses N-channel MOSFET as a switch and duty of this switch is controlled using voltage feed forward control method. The bias turns on the input side is used to provide a constant supply to the ICs. The outputs on the secondary side are rectified and filtered using diode rectifier and output filter circuits. To achieve good load regulation, mag-amp is used as post regulators. The maximum voltage requirement by digital unit is 6.6V, therefore over voltage protection circuit is designed with opto-coupler to limit output voltage to 120% of actual output.

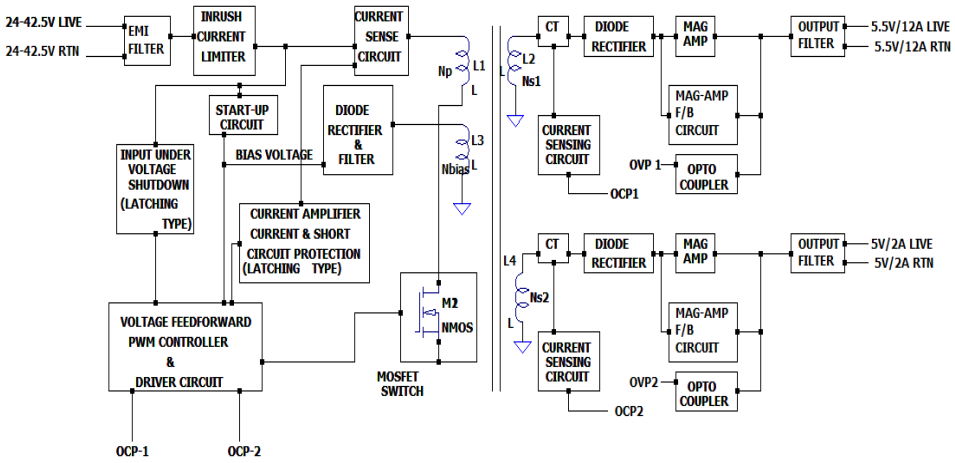

Fig 1. Block Diagram of the proposed converter

3. DESIGN PROCEDURE

In this section design of a) transformer b) criteria for selecting MOSFET switch c) snubber circuit selection d) output filter design e) mag-amp design have been explained. To make converter efficient, optimal selection of components are required.

3.1. Transformer Design

The area product calculation is used for selecting the transformer core. The optimum design is finally decided by the smaller size and lower power dissipation of transformer [3]

$$A_p = \frac{\sqrt{\text{Dmax}} \cdot P_{out} \cdot \left(1 + \frac{1}{\eta}\right)}{K_w \cdot J \cdot 10^{-6} F_{sw} \cdot \text{Bm}} \quad (1)$$

$$A_p = \frac{\sqrt{0.4} \cdot 76 \cdot \left(1 + \frac{1}{0.65}\right)}{0.35 \cdot 6 \cdot 10^{-6}\, 140.10^3 \cdot 0.2}$$

$$= 4150.17\ mm^4.$$

Where,

i) K_w : Window factor. ii) J: Current density A/mm^2. iii) F_{sw} : Switching frequency Hz. iv) D_{max} :Maximum duty cycle. v) **η**: Efficiency. vi) B_m: Maximum flux density T

An appropriate core will be selected which must have area product greater than the calculated Ap and better power handling capacity. From the ferrite core catalogue, selected **POT** core is **OR43019UG** which is having **A_L=6680nH/1000**Turns.

Primary turns are calculated from equation (2)

$$N_p = \frac{V_{in} \cdot \text{Dmax}}{B_m \cdot A_C \cdot 10^{-6} \cdot F_{sw}} \quad (2)$$

To know secondary turns, turns ratio to be calculated using formula (3)

$$\text{Tratio} = \frac{Np}{Ns} = \frac{Vout+Vd*Dmax}{Dmax*Vin(\min)} \quad (3)$$

Where,

i) Vd : Diode drop. ii)$Vin_{(min)}$: Minimum input voltage

Hence,

$$Ns = Tratio* Np \quad (4)$$

3.2. MOSFET SELECTION

Parameters to be considered for selection of MOSFET are drain to source voltage(V_{DS}), gate to source voltage(V_{GSth}) required to turn it on, continuous drain current(I_{Dmax}), drain to source ON resistance (R_{DS}(on)), input capacitances(C_{iss}) and output capacitances(C_{oss}). The stress on the MOSFET is calculated using equation (5) and suitable MOSFET is selected, which can withstand this stress.

$$V_{peak\text{-}MOSFET} = V_{in\text{-}max}\left(1+\frac{Npri}{Nreset}\right) \quad (5)$$

IRHM57260 is selected which has V_{DS} = 200V, $R_{DS(on)}$= 49mohm, I_{Dmax}=35A and $V_{GS(th)max}$=4V.

3.3. SNUBBER DESIGN

Parasitic inductances and resistances are associated with voltage spikes and current spikes. These will introduce electrical stresses on the switching devices. Hence snubbers are necessary to limit switching transients like dv/dt and di/dt and it also helps in lowering EMI by reducing ringing noise, that occurring due to leakage inductance of transformer. Lossless snubber (LCD snubber) is selected for recovering the leakage power loss from the MOSFET. It reduces switching off loss in mosfet. Lossless snubber contains two diodes, one inductor (Lsnubber) and one capacitor (Csnubber) (LCD). The suitable core for inductor is selected by calculating area product as shown in equation (6)

$$A_P = \frac{\text{Lsnubber} * Iout^2 * (1+\frac{K}{2})}{Kw*Bm*J*10^{-6}} = 16.411\text{mm}^4 \quad (6)$$

Where,

i) B_m : Max flux density. ii) K : Fill factor.

The selected core is **C055291A2 with A_L = 32nH/T^2**.

3.4. VOLTAGE FEED FORWARD CONTROL

In the conventional voltage feedback technique, the output voltage is compared with the reference wave and pulse width modulation is performed by comparing error signal with the constant ramp waveform. Though feedback technique is easier to design and analyse, the response is slow in regulating the duty cycle due to changes in input line voltage.

Hence voltage feed forward control is used to achieve fast dynamic response. In this control technique saw tooth wave is generated using RC network and this wave is compared with output of error amplifier which is taken as reference wave as shown in Fig 2 & 3. Hence duty ratio adjusted according to changes in input voltage[4].

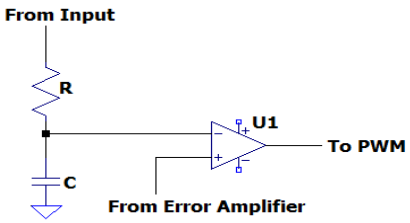

Fig 2. Duty cycle control using saw tooth and reference signal

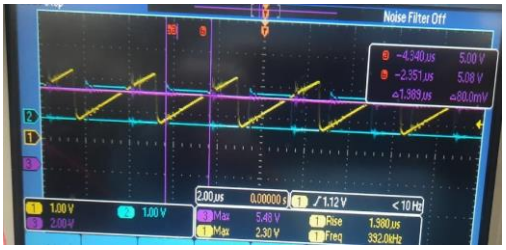

Fig.3 Duty cycles generated comparing saw tooth wave with output of error amplifier.

3.5. MAG-AMP DESIGN

A mag amp is a coil of wire wound on a core with a relatively square B-H characteristic [4]-[5]. This gives the coil two operating modes. When unsaturated, it does not allow current to flow and when saturated, it allows current to flow with zero voltage drop. The first task in design of mag amp is selection of proper core.

Core size is selected based on following area product method

$$A_p = \frac{Ax*A*}{\Delta B*K} 10^8 \ \ cm^4 \qquad (7)$$

Where,

i) ΔB : Flux excursion T ii) Ax : Wire area(One Conductor) in mm^2. iii) A: Required withstand area V-sec.

Selected core is **6-L2016-W763, Nanocrystalline Vitroperm 500Z, Square Loop Core**

3.6. OUTPUT FILTER DESIGN

The transformer's secondary voltage is rectified and filtered suitably to get the desired quality of output voltage waveform. The diode selected for rectification should have fast switching action and less reverse recovery time. Hence a suitable schottky diode is selected. The filter inductor and capacitor values need to be chosen optimally to arrive at a cost-effective, less bulky power supply. The filter capacitor merely supplies the ripple (ac) current of switching frequency. It has linear relation between the output voltage and the switch duty ratio, the inductor current is desired to be continuous. The L and C values are designed using following equations.

$$L = \frac{Vo*(1-Dmin)*Ts}{\Delta iL} \ H \qquad (8)$$

From above equation L1 = 12.1µH and L2 = 18µH are calculated values for master and slave outputs respectively.

$$C = \frac{1-Dmin}{8*L*Fsw^2*\delta Vo} \quad F \qquad (9)$$

Similarly C1 = 940µF and C2 = 470µF are the filter capacitances.

4. EXPERIMENTAL RESULTS

The Fig 4 a & b shows experimental set up and top view of the forward converter. The converter is powered up using DC voltage source and output is connected to an electronic load which measures the output voltage and load current. To measure ripple in the outputs a digital storage oscilloscope(DSO) is connected.

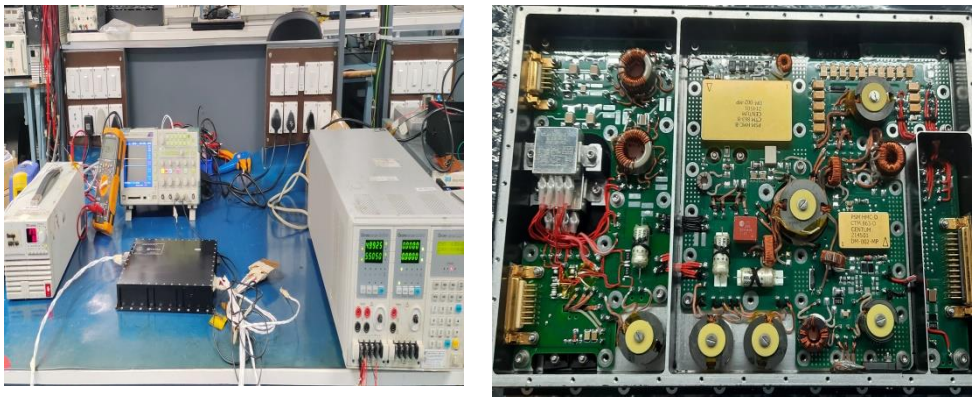

a b

Fig 4 a) Experimental Setup b) Top view of the forward converter.

The test results of the experimental prototype are shown in Table II, Table III, Table IV, Table V, Table VI and Table VII.

Table II. Outputs at full load(100%) condition

The measured outputs at full load condition are near to specified values and an efficiency greater than 65% is achieved.

V_{in} (V)	I_{in} (A)	V_{01} (V)	I_{o1} (A)	V_{02} (V)	I_{o2} (A)
24	4.653	5.468	12	4.971	2
36	3.111	5.472	12	4.974	2
42.5	2.656	5.547	12	4.98	2

Table III. Outputs at min load(10%) condition

Outputs at min load condition are measured and these values are nearly equal to the specified values since drop is less.

V_{in} (V)	I_{in} (A)	V_{01} (V)	I_{o2} (A)	V_{02} (V)	I_{o2} (A)
24	0.694	5.515	1.2	4.994	0.2
36	0.512	5.516	1.2	4.993	0.2
42.5	0.457	5.516	1.2	4.995	0.2

Table IV. Efficiency at different input voltages and full load

From table IV it can be seen that converter is designed to achieve efficiency greater than 65%.

Input Voltage(V)	Input Power(W)	Output Power(W)	Efficiency (%)
24	111.672	75.558	67.66
36	111.996	75.612	67.51
42.5	112.880	76.524	67.79

Table V. Line Regulation

With the use of feed-forward control method a line regulation <1% is achieved on both the outputs and it's shown in table IV.

	Line Regulation (%)	
Load	5.5V/12	5V/2A
100%	0.0144	0.0018
10%	0.0001	0.0002

Table VI. Load Regulation

The changes in the output voltage due to change in load current is less than the specified value (<±2%) and this is achieved by using post regulators mag-amps.

V_{in} (V)	Load Regulation (%)	
	5.5V/12A	5V/2A
24	0.0852	0.0046
36	0.0081	0.0038
42.5	0.0056	0.0003

Table VII. Ripple voltages in mV_{P-P}

The ripple is measured at full load condition for both the outputs and this value is less than the specified value($30mV_{p-p}$).

V_{in} (V)	5.5V	5V
24	18.8	13.6
36	13.2	20.8
42.5	20.4	14

The output ripple waveform at full load and maximum input voltage is shown in Fig 5. The ripple content in the first output is $18.8mV_{P-P}$ and in the second output is $13.6mV_{P-P}$, implying that the performance of the converter is improved with the use of output filter by limiting ripple value less than the specified value($30mV_{P-P}$).

For load transient response, the output-1 is kept at min load and output-2 load is varied from 50% to 100% and corresponding overshoot and undershoot are measured and these values are less than the specified value 275mV(5%) which is shown in below figure 6.

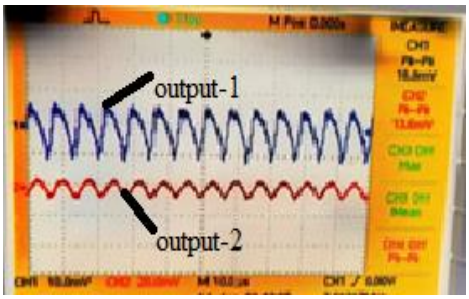

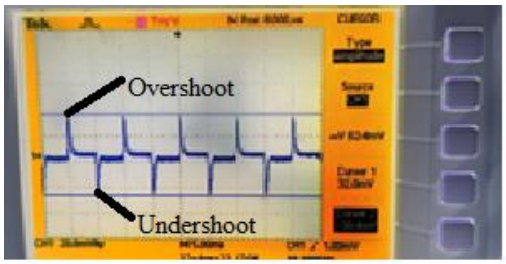

Fig.6 Load transient of output-2 at 36V

Fig 5 Output ripple waveform at full load and maximum input voltage(42.5V)

Output-1:5.5V/12A with Ripple =18.8mV

Output-2: 5V/2A with Ripple =13.6mV

input

Overshoot = 32mV ; Undershoot =30.4mV

Fig 7 shows the gate voltage and drain voltage values measured at nominal input voltage(36V). It can be seen that, the converter is operating at a specified frequency of 140kHz with a duty ratio of about 29.866%. With the use of LCD snubber, the spikes in the drain voltage(V_{DS}) are reduced and MOSFET can operate safely.

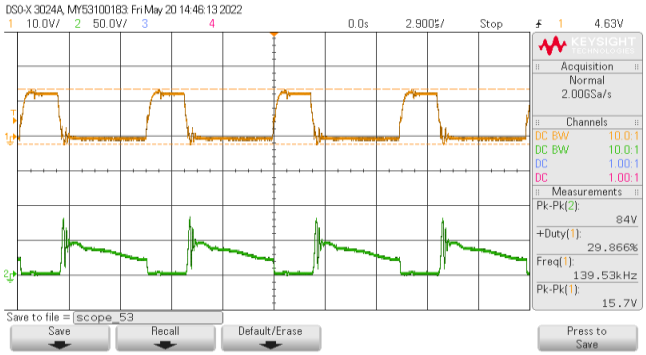

Fig 7. Gate voltage and Drain voltage(V_{DS}) at 36V input

7. CONCLUSION

The prototype model of the converter is designed and tested for all the selected specifications. Mag-amp regulation method gives better load regulation to regulate individual outputs. The voltage feed forward control method helps in meeting line regulation (< ±1%) as it gives fast dynamic response.

Acknowledgment

Authors are thankful to the Management, BMS Educational Trust, Principal and Vice Principal, BMS College of Engineering and Centum Electronics Ltd. for their continuous support.

REFERENCES

1] N. Lee, J. -Y. Lee, Y. -J. Cheon, S. -K. Han and G. -W. Moon, **"A High-Power-Density Converter With a Continuous Input Current Waveform for Satellite Power Applications,"** in IEEE Transactions on Industrial Electronics, vol. 67, no. 2, pp. 1024-1035, Feb. 2020, doi: 10.1109/TIE.2019.2898584

2] A. Bhat, K. U. Rao, Praveen P K, B. K. Singh and V. Chippalkatti, **"Multiple output forward DC-DC converter with regenerative snubber for space application,"** 2016 Biennial International Conference on Power and Energy Systems: Towards Sustainable Energy (PESTSE), 2016, pp. 1-5, doi: 10.1109/PESTSE.2016.7516487.

3] I. Shirsi, A. N. Nagashree, P. kumar Kulkarni, B. Singh, V. Chippalkatti and T. Kanthimathinathan, **"Self-resonant reset forward converter with dual-outputs for military application,"** 2012 IEEE International Conference on Power Electronics, Drives and Energy Systems (PEDES), 2012, pp. 1-6, doi: 10.1109/PEDES.2012.6484425.

4] A. Bhat, K. U. Rao, Praveen P K, B. K. Singh and V. Chippalkatti**,** "**Multiple output forward DC-DC converter with Mag-amp post regulators and voltage feedforward control for space application,"** 2016 Biennial International Conference on Power and Energy Systems: Towards Sustainable Energy (PESTSE), 2016, pp. 1-6, doi: 10.1109/PESTSE.2016.7516488.

5] Youhao Xi and P. K. Jain, **"A forward converter topology with independently and precisely regulated multiple outputs,"** in IEEE Transactions on Power Electronics, vol. 18, no. 2, pp. 648-658, March 2003, doi: 10.1109/TPEL.2003.809348..

6] N. Lee, T. -Y. Kim, J. -Y. Lee, S. -K. Han, T. -J. Chung and J. -D. Choi, "**Improved EMI noise performance by the reduced input ripple of the Satellite converter**," 2019 European Space Power Conference (ESPC), 2019, pp. 1-5, doi: 10.1109/ESPC.2019.8932057.

7] A. I. Pressman, **Switching Power Supply Design**. New York: McGrawHill, 1991, pp. 381–412**.**